REPORT DOCUMENTATION PAGE

Form Approved
OMB No. 0704-0188

1. REPORT DATE *(DD-MM-YYYY)*	**2. REPORT TYPE**	**3. DATES COVERED** *(From - To)*
November 2012	Technical Paper	November 2012-January 2013

4. TITLE AND SUBTITLE
Transition within a hypervelocity boundary layer on a 5-degree half-angle cone in freestream air/CO2 mixtures

5a. CONTRACT NUMBER
In-House

5b. GRANT NUMBER

5c. PROGRAM ELEMENT NUMBER

6. AUTHOR(S)
Joe Jewell, Ross Wagnild, Ivett Leyva, Graham Candler, Joe Shepherd

5d. PROJECT NUMBER

5e. TASK NUMBER

5f. WORK UNIT NUMBER
Q0AF

7. PERFORMING ORGANIZATION NAME(S) AND ADDRESS(ES)

Air Force Research Laboratory (AFMC)
AFRL/RQRE
4 Draco Drive.
Edwards AFB CA 93524-7160

8. PERFORMING ORGANIZATION REPORT NO.

9. SPONSORING / MONITORING AGENCY NAME(S) AND ADDRESS(ES)
Air Force Research Laboratory (AFMC)
AFRL/RQR
5 Pollux Drive
Edwards AFB CA 93524-7048

10. SPONSOR/MONITOR'S ACRONYM(S)

11. SPONSOR/MONITOR'S REPORT NUMBER(S)
AFRL-RQ-ED-TP-2012-460

12. DISTRIBUTION / AVAILABILITY STATEMENT
Distribution A: Approved for Public Release; Distribution Unlimited. PA#13023

13. SUPPLEMENTARY NOTES
Conference paper for the 51st AIAA Aerospace Sciences Meeting, Dallas, Texas, 7-10 January 2013.

14. ABSTRACT
The most significant instability mechanism which leads to laminar to turbulent transition in hypervelocity flow over cold, slender bodies, characteristic of high enthalpy facilities like the T5 hypervelocity shock tunnel at Caltech, is the so-called second or Mack mode, which depends upon the amplication of acoustic disturbances trapped in the boundary layer, as described by Mack (1984). At high Mach number (>4) and for cold walls, the first (viscous) mode is damped and higher inviscid modes are amplified, so that the second mode would be expected to be the only mechanism of linear instability leading to transition for a slender cone at zero angle of attack.

15. SUBJECT TERMS

16. SECURITY CLASSIFICATION OF:			**17. LIMITATION OF ABSTRACT**	**18. NUMBER OF PAGES**	**19a. NAME OF RESPONSIBLE PERSON**
					Ivett Leyva
a. REPORT	**b. ABSTRACT**	**c. THIS PAGE**			**19b. TELEPHONE NO** *(include area code)*
Unclassified	**Unclassified**	**Unclassified**	SAR	13	661-525-5817

Standard Form 298 (Rev. 8-98)
Prescribed by ANSI Std. 239.18

Transition within a hypervelocity boundary layer on a 5-degree half-angle cone in freestream air/CO_2 mixtures

Joseph S. Jewell[1]
California Institute of Technology, Pasadena, CA, 91125

Ross M. Wagnild[2]
Sandia National Laboratories, Albuquerque, NM, 87185

Ivett A. Leyva[3]
Air Force Research Laboratory, Edwards AFB, CA, 93536

Graham V. Candler[4]
University of Minnesota, Minneapolis, MN, 55455

Joseph E. Shepherd[5]
California Institute of Technology, Pasadena, CA, 91125

Nomenclature

A	=	amplitude of oscillation
f	=	frequency
h_{res}	=	reservoir enthalpy
M_e	=	boundary layer edge Mach number
P_{res}	=	reservoir pressure
$\dot{q}$	=	heat flux (transfer rate)
Re	=	Reynolds number
Re*	=	Reynolds number calculated at reference conditions
Re_1	=	unit Reynolds number
T_e	=	boundary layer edge temperature
T_w	=	wall temperature
u_e	=	boundary layer edge velocity
δ	=	boundary layer thickness

I. Introduction

THE most significant instability mechanism which leads to laminar to turbulent transition in hypervelocity flow over cold, slender bodies, characteristic of high enthalpy facilities like the T5 hypervelocity shock tunnel at Caltech, is the so-called second or Mack mode, which depends upon the amplication of acoustic disturbances trapped in the boundary layer, as described by Mack (1984). At high Mach number (>4) and for cold walls, the first (viscous) mode is damped and higher inviscid modes are amplified, so that the second mode would be expected to be the only mechanism of linear instability leading to transition for a slender cone at zero angle of attack.

Parametric studies in T5 by Germain (1993) and Adam (1997) on 5-degree half angle cones showed an increase in the reference Reynolds number Re* at the point of transition as reservoir enthalpy h_{res} increased. Germain and Adam also observed that flows of CO_2 transitioned at higher values of Re* than flows of air for the same h_{res} and P_{res}. Johnson et al. (1998) studied this effect with a linear stability analysis focused on the chemical

[1] Graduate Student, GALCIT, MC 205-45, Caltech. AIAA Student Member.
[2] Senior Member, Technical Staff, Sandia National Laboratories. AIAA Member.
[3] Sr. Aerospace Engineer, Air Force Research Laboratory. AIAA Associate Fellow.
[4] Professor, University of Minnesota. AIAA Fellow.
[5] Professor, GALCIT, MC 105-50, Caltech. AIAA Senior Member.

composition of the flow, and found an increase in transition Reynolds number with free-stream total enthalpy, and further found the increase to be greater for gases with lower vibrational energies, such as CO_2. In fact, with the assumption of a transition N-factor of 10 that was made at the time, none of the CO_2 cases computed by Johnson et al. transitioned at all. These effects lead Fujii and Hornung (2001) to further investigate that the delay in transition was due to the damping of acoustic disturbances in non-equilibrium relaxing gases by vibrational absorption. Fujii and Hornung estimated the most strongly amplified frequencies for representative T5 conditions and found that these agreed well with the frequencies most effectively damped by non-equilibrium CO_2. This suggests that the suppression of the second mode through the absorption of energy from acoustic disturbances through vibrational relaxation is the dominant effect in delaying transition for high-enthalpy carbon dioxide flows.

Numerous studies have been made on inhibiting the second mode, and therefore preventing or delaying transition through the suppression of acoustic disturbances within the boundary layer; see Fedorov et al. (2001) and Rasheed (2001) for work focused on absorbing acoustic energy using porous walls. Another approach to suppressing the pressure waves that lead to transition centers around altering the chemical composition within the boundary layer to include species capable of absorbing acoustic energy at the appropriate frequencies. Efforts in this area to date have included preliminary experimental work on mixed free-stream flows, e.g. Leyva (2009), computations, e.g. Wagnild et al. (2010) and Wagnild (2012), and experiments with direct injection of absorptive gases into the boundary layer, e.g. Jewell et al. (2011). The present aim is to confirm and extend these studies both computationally and experimentally by considering transition within a hypervelocity boundary layer on a 5-degree half-angle cone in freestream mixtures of air and carbon dioxide.

II. Background

By assuming that the boundary layer acts as an acoustic waveguide for disturbances (see Fedorov (2011) for a schematic illustration of this effect), the frequency of the most strongly-amplified second-mode disturbances in the boundary layer may be estimated, as shown in Stetson (1992), as:

$$f \approx 0.8 \frac{u_e}{2\delta}$$

Here δ is the boundary layer thickness and u_e is the velocity at the boundary layer edge. For a typical T5 condition in air, with enthalpy of 10 MJ/kg and stagnation pressure of 50 MPa, the boundary layer thickness is on the order of 1.5mm and the edge velocity is 4000 m/s. This indicates that the most strongly amplified frequencies are in the 1 MHz range. This is broadly consistent with the results of Fujii and Hornung (2001).

Kinsler et al. (1982) provide a good general description of the mechanisms of attenuation of sound waves in fluids due to molecular exchanges of energy within the medium. The relevant exchange of energy for carbon dioxide in the boundary layer of a thin cone at T5-like conditions is the conversion of molecular kinetic energy (e.g. from compression due to acoustic waves) into internal vibrational energy. In real gases, molecular vibrational relaxation is a non-equilibrium process, and therefore irreversible. This absorption process has a characteristic relaxation time.

The problem of sound propagation, absorption, and dispersion in a dissociating gas has been treated from slightly different perspectives by Clarke and McChesney (1964), Zeldovich and Raizer (1967), and Kinsler et al. (1982). However, in non-equilibrium flows when the acoustic characteristic time scale and relaxation time scale are similar, some finite time is required for molecular collisions to achieve a new density under an acoustic pressure disturbance. This results in a limit cycle, as the density changes lag the pressure changes. The area within the limit cycle is related to energy absorbed by relaxation. Energy absorbed in this way is transformed into heat and does not contribute to the growth of acoustic waves (Leyva et al. 2009).

Carbon dioxide, a linear molecule, has four normal vibrational modes. The first two, which correspond to transverse bending are equal to each other, and have characteristic vibrational temperatures $\Theta_1 = \Theta_2 = 960.1$ K. The third mode, corresponding to asymmetric longitudinal stretching has $\Theta_3 = 1992.5$ K, and the fourth mode, corresponding to symmetric longitudinal stretching, has $\Theta_4 = 3380.2$ K.

Camac (1966) showed that the four vibrational modes for carbon dioxide all relax at the same rate, and proposed this simplified formula to calculate vibrational relaxation time, as reproduced in Fujii and Hornung (2001):

$$\ln\left(A_4 \tau_{CO_2} p\right) = A_5 T^{-1/3}$$

Here A_4 and A_5 are constants given by Camac for carbon dioxide as $A_4 = 4.8488 \times 10^2$ $Pa^{-1}s^{-1}$ and $A_5 = 36.5$ $K^{1/3}$. Using the constants suggested by Camac, with p = 35kPa and T = 1500K, which are consistent with a typical T5

condition with enthalpy 10 MJ/kg and stagnation pressure 50 MPa, we find vibrational relaxation time τ_{CO_2} = 1.43 x 10^{-6} s, which indicates that frequencies around 700KHz should be most strongly absorbed at these conditions. This is, again, broadly similar to the results of Fujii and Hornung (2001), who computed curves at 1000K and 2000K with peaks bracketing 700kHz.

Thus, in a flow of gas that absorbs energy most efficiently at frequencies similar to the most strongly amplified frequencies implied by the geometry of the boundary layer, laminar to turbulent transition should be delayed. We show computationally that on a slender cone at T5-like conditions, carbon dioxide/air mixtures are such flows, and perform a series of experiments to confirm this effect.

III. Experimental Model

The facility used in all experiments for the current study is the T5 hypervelocity reflected shock tunnel; see Hornung (1992) and Hornung and Belanger (1990). The model is a 5 degree half-angle aluminum cone similar to that used in a number of previous experimental studies in T5, 1m in length, and is composed of three sections: a sharp tip fabricated of molybdenum, a mid-section containing a porous gas-injector section (in the present experiments this section is a smooth, solid piece of plastic), and the main body instrumented with a total of 80 thermocouples evenly spaced at 20 lengthwise locations. These thermocouples have a response time on the order of a few microseconds (Marineau and Hornung 2009) and have been successfully used for boundary layer transition location in Adam (1997) and Rasheed (2001). The conical model geometry was chosen because of the wealth of experimental and numerical data available with which to compare the results from this program. Two photographs of the cone model are shown in Figure 1.

IV. Computational Method

In order to obtain the flow properties over the test cone, we start with the flow properties in the tunnel reservoir, which serves as the inflow for the nozzle flow simulations. The reservoir conditions are obtained by solving for chemical and thermal equilibrium at the specified reservoir pressure and enthalpy using the Chemical Equilibrium with Applications (CEA) code. These conditions are allowed to expand through the nozzle using the CFD solver described below. For the current computational analysis, it is assumed that the boundary layer on the nozzle walls becomes turbulent in the reservoir and remains in this state for the remainder of the nozzle. A second CFD solver is used to simulate the flow over the test cone, also described below. The freestream properties over the cone are approximated by sampling the nozzle flow at the centerline of the nozzle exit. A seven species chemistry model including CO2, CO, N2, O2, NO, N, O is used to approximate the flow through the nozzle as well as over the cone for all conditions tested. In all cases the wall temperature for the nozzle and cone walls is 297 K. Also for the computations, the cone nose has been approximated as sharp, with a nose radius of 0.0125mm.

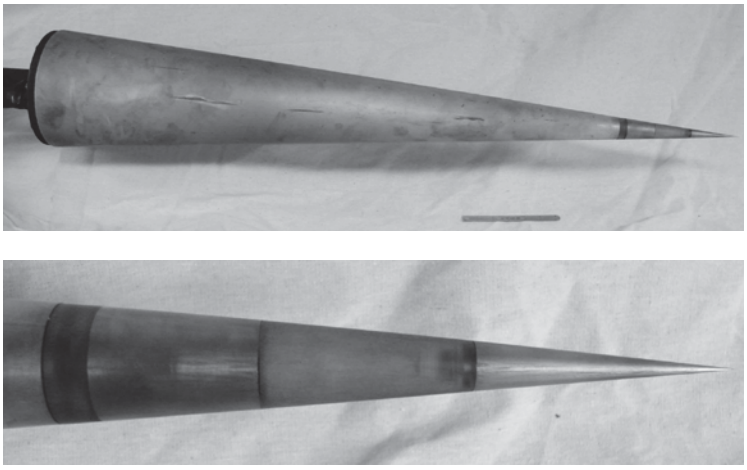

Figure 1. Top: Aluminum cone, 1m in length, instrumented with 80 thermocouples in 20 rows. Bottom, from right to left: molybdenum tip, plastic holder with 316L stainless steel 10 micron porous section, aluminum cone body.

We simulate the flow through the nozzle by solving the reacting, axi-symmetric, two-dimensional Navier-Stokes equations with a structured CFD solver as described in Candler (2005) and Wagnild (2012). The solver uses an excluded volume equation of state in order to properly capture the variation in gas properties at high pressure. The inviscid fluxes are calculated using the modified Steger-Warming flux vector splitting method and are second-order accurate with a MUSCL limiter as the TVD scheme. The viscous fluxes are second-order accurate. The time advancement method is the implicit, first-order DPLR method. The turbulent boundary layer flow is modeled using

the one equation, Spalart-Allmaras model with the Catrix-Aupoix compressibility correction. The nozzle flow is calculated on a single-block, structured grid with dimensions 492 cells by 219 cells in the streamwise and wall-normal directions.

The mean flow for the stability analysis is calculated using a structured, axi-symmetric CFD solver, which solves the reacting Navier-Stokes equations and is part of the STABL software suite (Johnson 2000). This flow solver is also based on the finite-volume formulation and is similar to the one used to simulate the nozzle flow with the exception of the excluded volume equation of state. This specialized equation of state is not necessary for this solver because the static pressure over the cone is not sufficiently high to require an altered equation of state. The mean flow is computed on a single-block, structured grid with dimensions of 1001 cells by 301 cells in the streamwise and wall-normal directions.

The stability analyses are performed using the PSE-Chem solver, which is also part of the STABL software suite. PSE-Chem (Johnson and Candler 2005) solves the reacting, two-dimensional, axi-symmetric, linear parabolized stability equations to predict the amplification of disturbances as they interact with the boundary layer. The PSE-Chem solver includes finite-rate chemistry and translational-vibrational energy exchange. The parabolized stability equations predict the amplification of disturbances as they interact with the boundary layer. The transition location is then predicted using the semi-empirical e^N approach, in which transition is assumed to occur when a disturbance has grown by a factor of e^N from its initial amplitude. The critical value of N should depend on the disturbance environment, therefore, N must be calibrated for a particular wind tunnel facility. Conventional, non-quiet, supersonic wind tunnels have been generally understood to have a transition N factor in the range of 5-6 (Schneider 2001). Both the mean flow and stability analysis solvers in STABL are capable of selectively freezing both chemical reactions and molecular vibration, allowing for the determination of internal molecular effects on boundary layer disturbances.

V. Computational Results

Using the methods described above, seven test gas mixtures are simulated, each at three different freestream conditions. The gas mixtures are given based on the mass fraction of carbon dioxide in the mixture and are 0.0, 0.1, 0.2, 0.3, 0.5, 0.75, 1.0. The freestream conditions are chosen based on the reservoir pressure and the reservoir enthalpy and are 10 MJ/kg and 50 MPa, 7 MJ/kg and 40 MPa, and 5 MJ/kg and 30 MPa. For each gas mixture, the formation enthalpy of the mixture is omitted from the reservoir enthalpy in order to make a proper comparison between test cases. To determine the predicted transition location on the test cone, a transition N factor of 5 is chosen. The transition locations along the cone surface are extracted from the results of the stability analyses of each case and are compiled in Figure 2. Previous work (Johnson et. al 1998, Fujii and Hornung 2003, Leyva et al. 2009) has indicated the potential benefits of having carbon dioxide in the boundary layer for transition delay. One objective of the current computations is to determine the regime in which a transition delay can be obtained. The data in Figure 2 show that an increase of the mass fraction of carbon dioxide in the 5 MJ/kg case has only a small effect on the transition location. At 7 MJ/kg, the transition location moves toward the rear of the cone by about 5 cm at 100% CO_2. The 10 MJ/kg case results in the largest shift in the transition location, approximately 66 cm at 100% CO_2, indicating that carbon dioxide has a large potential for transition delay in this enthalpy range.

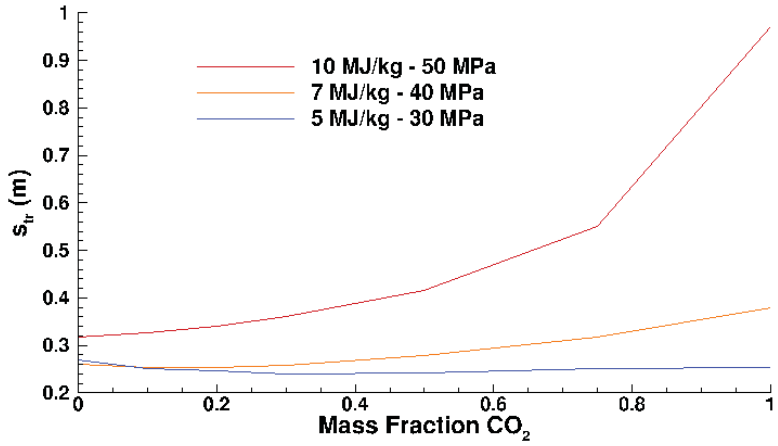

Figure 2. Comparison of the transition location based on a critical N factor of 5 versus mass fraction of CO_2 for each of the three freestream conditions.

Using the ability of the stability analysis in STABL to freeze the chemical and vibrational rate processes, we can determine the effect of these rate processes on the damping of second mode disturbances. An example of this type of calculation is demonstrated by comparing the transition location for a fully reacting stability analysis and a frozen gas stability analysis for the 10 MJ/kg case, as shown in Figure 3. Using a reacting mean flow and a frozen gas stability analysis, the data show that adding carbon dioxide promotes transition. When the chemical and vibrational rate processes are included in the stability analysis, the transition location moves further down the cone due to carbon dioxide's ability to damp boundary layer disturbances. By calculating the change in transition location, we can compare the effectiveness of disturbance damping in each of the three freestream conditions, shown in Figure . For all cases tested, the addition of chemical and vibrational rate processes results in a shift in the transition location towards the rear of the cone that increases with an increasing mass fraction of carbon dioxide in the test gas. From these data, it becomes clear that the damping ability of carbon dioxide is most effective for the 10 MJ/kg case. Interestingly, the addition of carbon dioxide in the 5 MJ/kg case has little or no effect as indicated in Figure , despite the disturbance damping ability of molecular vibration demonstrated in Figure 4. This is consistent with the diminishing of vibrational and chemical non-equilibrium with decreasing reservoir enthalpy.

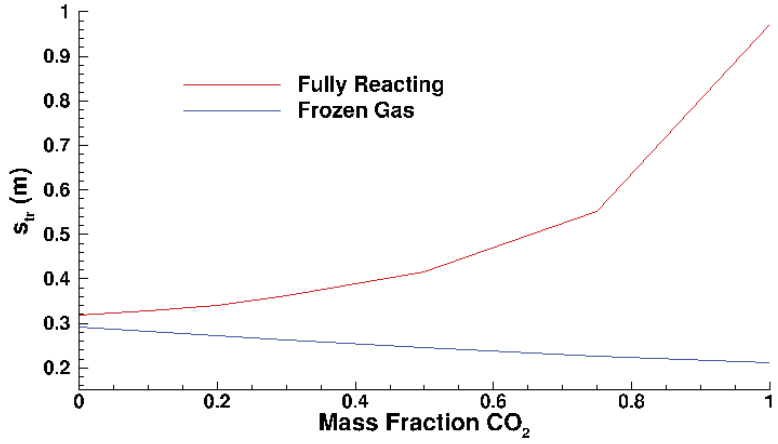

Figure 3. A comparison of the transition location versus mass fraction of CO_2 based on a N factor of 5 between a fully reacting and a frozen gas stability analysis at 10 MJ/kg and 50 MPa. The shift in transition location at all mass fractions is due to the presence of molecular vibration in the stability analysis.

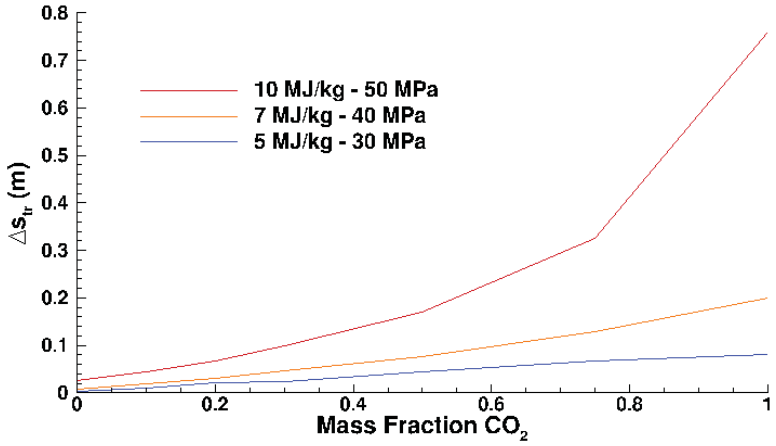

Figure 4. Comparsion of the change in transition location due to vibrational relaxation versus mass fraction of CO_2 based on a transition N factor of 5 for each of the three freestream conditions tested. The shift in transition location at all mass fractions is due to the presence of chemical and vibrational rate processes in the stability analysis.

VI. Experimental Results

Although there have been several previous experimental campaigns on transition in T5 (Germain 1993, Adam 1997, Leyva et al. 2009, Jewell et al. 2011), based on recent experience with T5 operations, it is desirable to conduct new experiments with special attention paid to repeatability and cleanliness of the tunnel. Based on the computations described above, we choose four carbon dioxide/air gas mixtures which were tested in T5 on the 5-degree half-angle cone, with reservoir enthalpies varying from 7.03 – 9.67 MJ/kg and reservoir pressures, held as consistently as possible near 58 MPa, but varying from 53.4 – 61.9 MPa, to attempt to reproduce the largest shift in transition location implied by the computations. The gas mixtures, by mass fraction of carbon dioxide in the mixture, are 0.0 (e.g. all air), 0.5, 0.75, 1.0. A summary of run conditions and results is presented in Table 1.

One example of results from the present tests, shot 2744 in air, is shown in Figure 5. Normalized heat-transfer results at 7.68 MJ/kg and 60.7 MPa are presented. The circles are time-averaged measurements from each of 80 thermocouples for the ~1ms steady flow time, and the bars represent the root mean squared values from each sensor. The RMS bars are initially small in the laminar zone as the heat transfer levels are consistently at the laminar value, increase in size in the transitional zone as the flow becomes intermittent, and then decrease in size again as the flow approaches the fully turbulent zone and heat transfer levels are consistently near the turbulent value. A slight drop-off from the fully turbulent value is observed in the last two rows of thermocouples, as they are positioned near the maximum extent of the T5 test rhombus and may intersect with the expansion fan emanating from the lip of the nozzle. For this experiment, transition is observed at 52 cm from the tip of the cone, which is much greater than the predicted value for a typical noisy flow assumption of N=5.

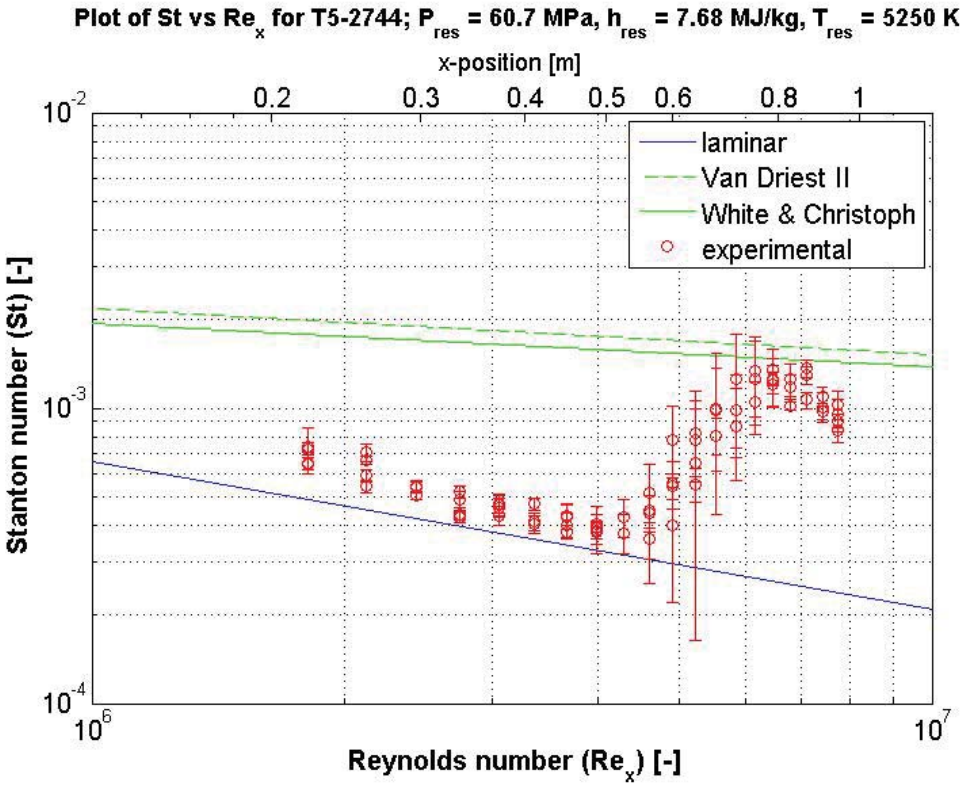

Figure 5. Time-averaged non-dimensional plot of heat transfer results in terms of Stanton number vs. Reynolds number for T5 shot 2744 in 100% air, with the laminar similarity correlation indicated in blue and two common turbulent correlations in green. The bars on each point represent the RMS values of each thermocouple's signal, and transition onset occurs at Re = 4.3 × 10^6, which is 0.52m from the tip of the cone.

Figure 6 presents four N-factor curves along the surface of the cone as computed by STABL for four different 100% air shots. These computations indicate that transition over the range of conditions investigated in air happens at N=10 or greater. The present experimental results are a closer match to the present computations than an earlier study (Johnson et al. 1998) which used a similar methodology with the assumption that transition occurred at N=10, and found that transition Reynolds numbers were overpredicted by a factor of 2 when compared experimentally with T5 experiments performed by Adam (1997). The current measurement of N=10 may be at least partially due to the suppression of particulate-induced transition through much more thorough cleaning of the compression tube, shock tube, nozzle, and other wetted components of T5 than has been standard practice in the past.

Flow conditions in T5 are calculated from three tunnel measurements: the shock speed, initial shock tube fill pressure and composition, and reservoir pressure at the end of the shock tube during the run time. Shock speed is measured by two time of arrival pressure transducers positioned 2.402m apart, with an approximate measurement uncertainty of 8 × 10^{-6} s. The uncertainty in the shock speed measurement thus increases as the measured time of arrival difference decreases. At a shock speed of 3000 m/s, typical for the present study, the uncertainty is ±30 m/s. The shock tube fill pressure uncertainty is ±0.05 kPa, and the measured reservoir pressure uncertainty is typically ±4 MPa. Uncertainties on the calculated quantities, including those represented by the error bars in Figures 7-9, are estimated by perturbing Cantera (Goodwin 2009) condition computations within the range of the uncertainties on the measured shock speed, reservoir pressure, and initial shock tube pressure.

Transition x-locations over the range of enthalpies for each gas mixture are summarized in Figure 7. A strong correlation between reservoir enthalpy and transition location is apparent for all gas mixtures, and delays of up to 30% (at 9.2 MJ/kg) are observed for flows containing CO_2 compared to experiments in pure air.

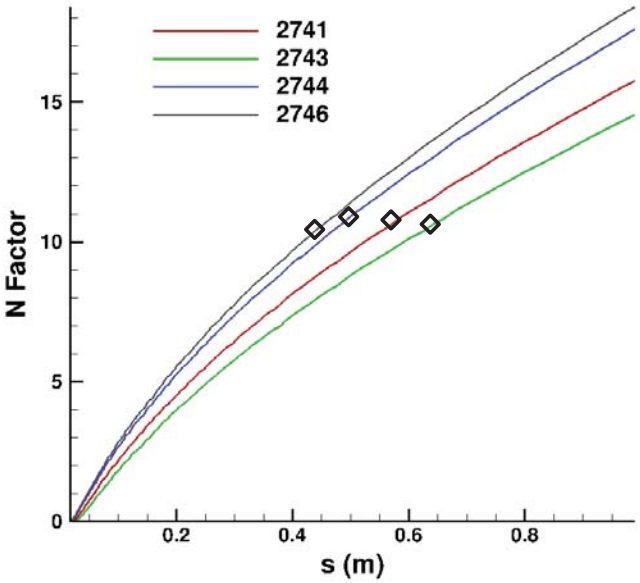

Figure 6. N-factor vs. distance along the surface of the cone as computed by STABL for the conditions of four of the present air experiments (T5 shots 2741, 2743, 2744, and 2746). The experimentally measured transition locations are indicated by hollow black diamonds on each curve, and indicate a transition N-factor between 10.2 and 10.8.

Figure 8 presents the same data in terms of the Reynolds number evaluated at edge conditions:

$$\mathrm{Re}_{tr} = \frac{\rho_e u_e x_{tr}}{\mu_e}$$

While experiments with CO_2 in the free stream remain distinct from air tests, the results within each gas mixture condition seem to be flatter, weakening the trend with reservoir enthalpy seen in the x-location data seen in Figure 7. In terms of Re, delays up to 38% (at ~9.2 MJ/kg) are observed for the measured transition location in flows containing CO_2 compared to experiments in pure air.

Experiments by Adam (1997) showed that computing the transition Reynolds number at reference conditions strongly separated pure CO_2 results from pure air and N_2 data. The Dorrance (1962) reference temperature has the same form as the Eckert reference temperature but may be used for other gases:

$$\frac{T^*}{T_e} = \frac{1}{2} + \frac{\gamma - 1}{2}\frac{\sqrt{\mathrm{Pr}}}{6} M_e^2 + \frac{1}{2}\frac{T_w}{T_e}$$

The Dorrance temperature is used to calculate Re*, the Reynolds number with density and viscosity evaluated at reference conditions:

$$\mathrm{Re}^*_{tr} = \frac{\rho^* u_e x_{tr}}{\mu^*}$$

The results of the present study calculated in terms of Re* are in Figure 9. This approach effectively correlates observed transition locations for each gas mixture across the entire range of enthalpies examined, clearly separating air, CO_2 and mixture cases. In terms of Re*, delays up to 140% (at ~9.2 MJ/kg) are observed for the measured transition location in flows containing CO_2 compared to experiments in pure air.

Experiment	CO_2 Mass Fraction	h_{res} [MJ/kg]	P_{res} [MPa]	x_{trans} [m]	Re_{trans} [-]
2720	1	9.65	59.3	>0.824	$>5.31 \times 10^6$
2729	0.50	8.45	57.7	0.721	5.01×10^6
2730	0.50	7.80	58.1	0.639	4.90×10^6
2731	0.75	8.96	59.0	>0.827	$>5.60 \times 10^6$
2732	0.50	7.84	57.0	0.714	5.25×10^6
2733	1	7.03	56.6	0.602	5.13×10^6
2736	0.75	7.72	57.0	0.674	5.16×10^6
2737	0.75	7.10	56.1	>0.789	$>6.38 \times 10^6$
2738	0.75	8.33	56.6	0.733	5.13×10^6
2739	0	8.03	57.5	0.547	3.98×10^6
2740	0	7.97	57.3	0.544	3.96×10^6
2741	0	8.34	56.9	0.567	3.89×10^6
2742	0	8.64	55.7	0.581	3.80×10^6
2743	0	9.09	56.3	0.639	3.94×10^6
2744	0	7.68	60.7	0.522	4.27×10^6
2745	1	9.67	58.5	>0.797	$>5.00 \times 10^6$
2746	0	7.38	61.9	0.429	3.72×10^6
2747	1	9.36	60.3	>0.855	$>5.75 \times 10^6$
2749	0.50	9.59	60.4	0.829	5.19×10^6
2750	0.50	9.00	60.0	0.829	5.58×10^6
2751	1	9.04	60.2	>0.835	$>5.75 \times 10^6$
2754	1	9.41	53.4	>0.805	$>4.90 \times 10^6$
2756	1	8.72	57.5	>0.821	$>5.62 \times 10^6$

Table 1. Run conditions and results included in the present study. In the last two columns, the > symbol indicates that the flow was laminar to the last measurable thermocouple location, which is recorded.

VII. Conclusions and Future Work

Consistent transition N-factors greater than 10 have been found over a 5 degree half-angle in the T5 hypervelocity shock tunnel for air flows with reservoir enthalpies above 7.68 MJ/kg. Likewise, for CO_2 and mixture measurements at equivalent enthalpy conditions, results above N=7 and N=9 have been calculated. Transition is delayed in terms of physical x-location, Reynolds number, and the Reynolds number calculated in terms of reference conditions, and this delay appears to become more pronounced as the mass fraction of CO_2 within the boundary layer increases. This suggests that the suppression of the second mode through the absorption of energy from acoustic disturbances through vibrational relaxation is a mechanism for delaying transition both in high-enthalpy carbon dioxide flows and, more usefully, high-enthalpy flows consisting of a mixture of CO_2 and air.

These results are quite promising. Future work will include studies using premixed CO_2 and air to fill the shock tube to address concerns about completeness of the gaseous mixing process prior to each experiment, studies in gases other than CO_2, and ultimately continuation of the boundary-layer injection work begun in Jewell et al. 2011.

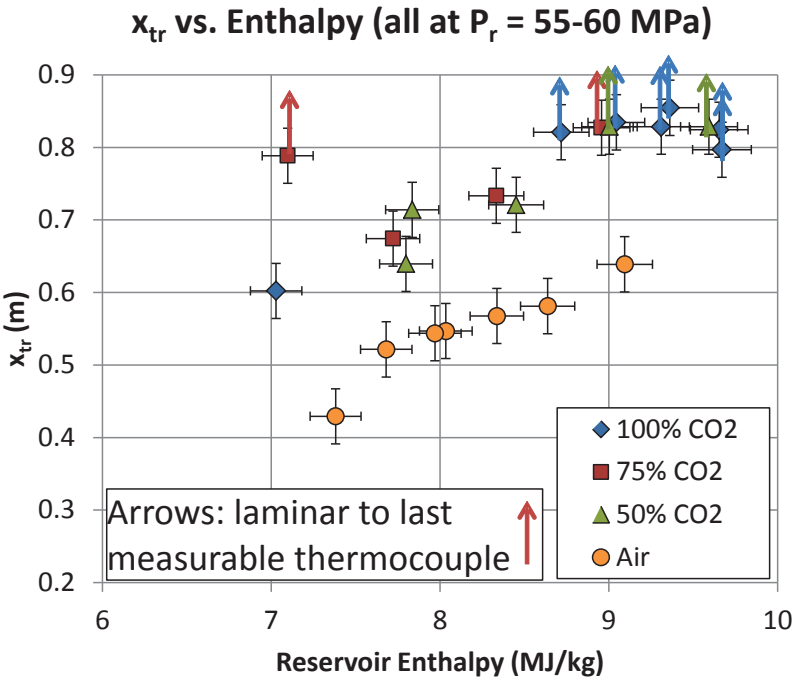

Figure 7. Location of transition on the cone surface vs. reservoir enthalpy, with reservoir pressure held near 58 MPa for all experiments.

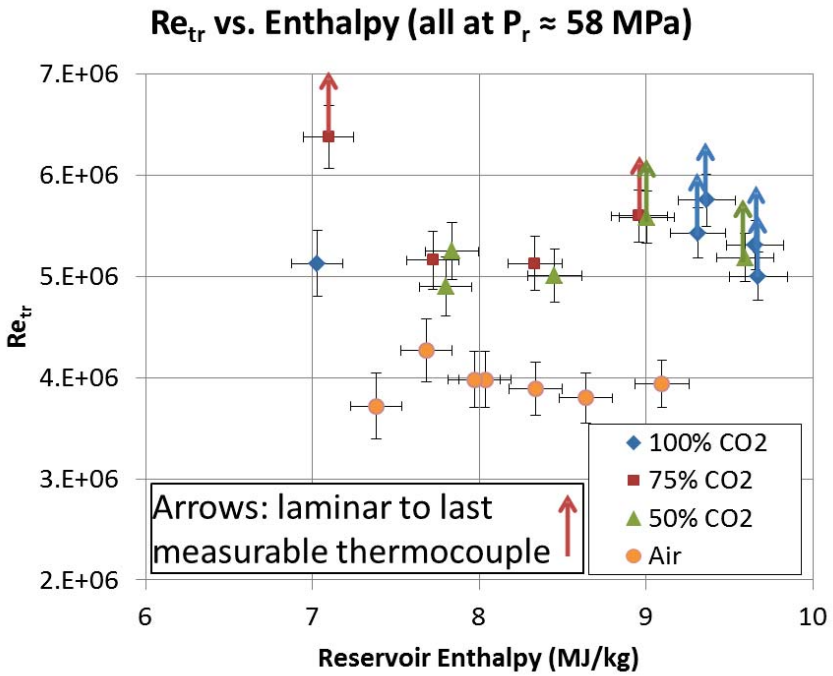

Figure 8. Reynolds number at transition (evaluated at edge conditions) vs. reservoir enthalpy, with reservoir pressure held near 58 MPa for all experiments.

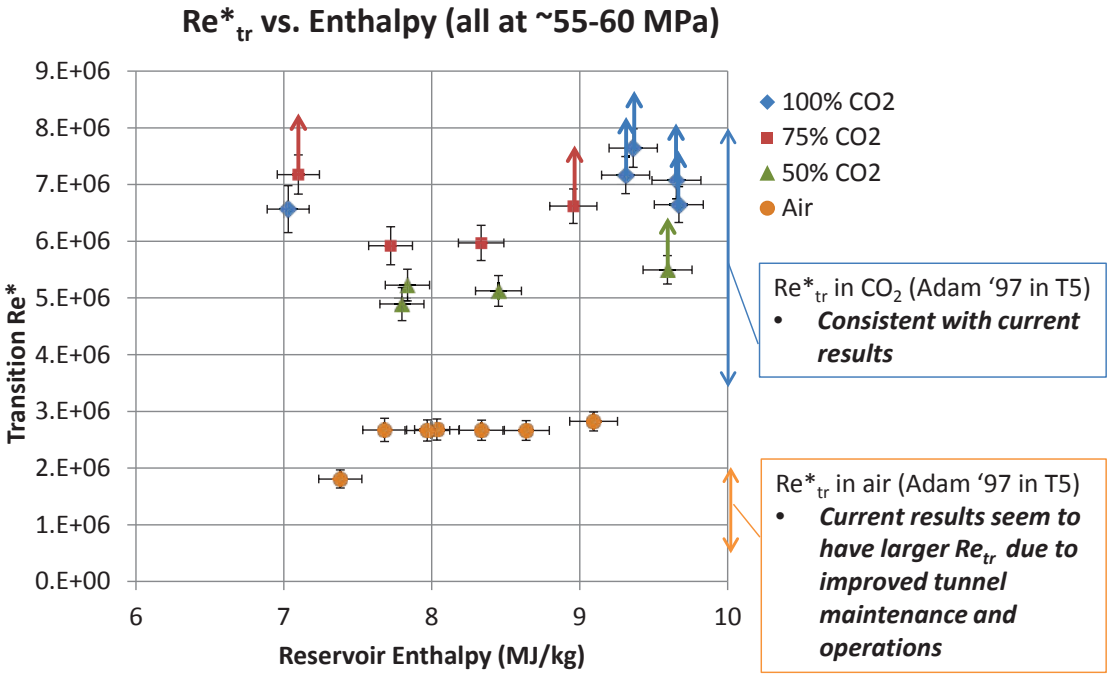

Figure 9. Reynolds number at transition (evaluated at Dorrance reference conditions) vs. reservoir enthalpy, with reservoir pressure held near 58 MPa for all experiments. The range of results for Re* presented in Adam (1997) are included for comparison.

Acknowledgments

The authors thank Mr. Nick Parziale for his assistance in running T5, Mr. Bahram Valiferdowsi for his work with design, fabrication, and maintenance, and Prof. Hans Hornung for his advice and support. The experimental portion of this project was sponsored by the Air Force Office of Scientific Research under award number FA9550-10-1-0491 and the NASA/AFOSR National Center for Hypersonic Research. The views expressed herein are those of the authors and should not be interpreted as necessarily representing the official policies or endorsements, either expressed or implied, of AFOSR or the U.S. Government.

References

Adam, P.H., *Enthlapy Effects on Hypervelocity Boundary Layers*. PhD Thesis, California Institute of Technology, Pasadena, CA, 1997.

Camac, M. "CO2 relaxation processes in shock waves." In J.G Hall, editor, Fundamental Phenomena in Hypersonic Flows, pp. 195-218. Ithaca: Cornell University Press (1966).

Clarke, J.F. and McChesney, M. *Dynamics of Relaxing Gases*. Butterworths (1976). Chapter 6.

Candler, G. V. "Hypersonic Nozzle Analysis Using an Excluded Volume Equation of State", Paper 2005-5202, AIAA, June 2005.

Dorrance, W.H. (1962) *Viscous hypersonic flow: theory of reacting and hypersonic boundary layers*. McGraw-Hill, pp. 134-140.

Fedorov A.V., Malmuth N.D., Rasheed A. and Hornung H.G. (2001) Stabilization of hypersonic boundary layers by porous coatings. AIAA Journal, Vol. 39, No. 4.

Fedorov, A.V. "Transition and stability of high-speed boundary layers." Annual Review of Fluid Mechanics, Vol. 43, pp. 77-95, 2011.

Fujii, K. and Hornung, H.G. "A procedure to estimate the absorption rate of sound propagating through high temperature gas". GALCIT Report FM 2001.004. August 8, 2001.

Fujii, K. and Hornung, H.G. “Experimental Investigation of High-Enthalpy Effects on Attachment-Line Boundary-Layer Transition”. AIAA Journal. Vol. 41, No. 7, July 2003.

Germain, P. *The Boundary Layer on a Sharp Cone in High-Enthalpy Flow*. PhD Thesis, California Institute of Technology, Pasadena, CA, 1993.

Goodwin, D. “Cantera: An object-oriented software toolkit for chemical kinetics, thermodynamics, and transport processes.” Caltech, Pasadena, 2009. [Online]. Available: http://code.google.com/p/cantera

Hornung, H.G. and Belanger, J. “Role and techniques of ground testing simulation of flows up to orbital speeds.” 1990. AIAA 90-1377.

Hornung, H.G. “Performance data of the new free-piston shock tunnel at GALCIT.” 1992. AIAA 92-3943.

Jewell, J.S., I.A. Leyva, N.J. Parziale, J.E. Shepherd. “Effect of Gas Injection on Transition in Hypervelocity Boundary Layers.” Proceedings of the 28th International Symposium on Shock Waves, July 2011, Manchester, UK.

Johnson, H.B., *Thermochemical Interactions in Hypersonic Boundary Layer Stability*. PhD Thesis, University of Minnesota, 2000.

Johnson, H.B., and Candler, G.V. “Hypersonic Boundary Layer Stability Analysis Using PSE-Chem.” Paper 2005-5023, AIAA, June 2005.

Johnson, H.B., Seipp, T.G, and Candler, G.V. “Numerical study of hypersonic reacting boundary layer transition on cones”. Phys. Fluids 10, 2676 (1998).

Kinsler, L.E, Frey, A.R, Coppens, A.B, Sanders, J.V. *Fundamentals of Acoustics (Third Edition)*, pp. 141-157. New York: Wiley (1982).

Leyva, I.A., S.J. Lawrence, A. WK. Beierholm, H.G. Hornung, R. Wagnild, G. Candler. “Transition delay in hypervelocity boundary layers by means of CO2/acoustic instability interactions”. January 2009. AIAA 2009-1287.

Mack L.M. Boundary-layer stability theory. Special Course on Stability and Transition of Laminar Flow. 1984. AGARD Report 709.

Marineau, E., and Hornung, H., “Modeling and Calibration of Fast-Response Coaxial Heat Flux Gages,” AIAA Paper 2009-737, 47th AIAA Aerospace Sciences Meeting, Orlando, FL, January 2009.

Rasheed, A., *Passive hypervelocity boundary layer control using an acoustically absortive surface.* PhD Thesis, California Institute of Technology, Pasadena, CA, 2001.

Schneider, S.P. “Effects of High-Speed Tunnel Noise on Laminar-Turbulent Transition,” Journal of Spacecraft and Rockets, Vol. 38, No. 3, May–June 2001.

Stetson, K.F. “Hypersonic boundary layer transition.” In JJ Bertin, J Periaux, J Ballmann, editors, *Advances in Hypersonics: Defining the Hypersonic Environment, Volume 1*. p. 334. Boston: Birkhauser (1992).

Wagnild, R.M. *High Enthalpy Effects on Two Boundary Layer Disturbances in Supersonic and Hypersonic Flow*. PhD Thesis, University of Minnesota, Minneapolis, MN, 2012.

Wagnild R.M., Candler G.V., Leyva I.A., Jewell J.S. and Hornung H.G. “Carbon Dioxide Injection for Hypervelocity Boundary Layer Stability”. AIAA 2010-1244.

Zeldovich, Y.A., and Raizer, Y.P. *Physics of Shock Waves and High-Temperature Hydrodynamic Phenomenon*. New York: Academic Press (1967), pp. 553-564.